
OTTER-KNOWLEDGE: BENCHMARKS OF MULTIMODAL KNOWLEDGE GRAPH REPRESENTATION LEARNING FROM DIFFERENT SOURCES FOR DRUG DISCOVERY

Hoang Thanh Lam, Marco Luca Sbodio, Marcos Martínez Gallindo, Mykhaylo Zayats, Raúl Fernández-Díaz, Víctor Valls, Gabriele Picco, Cesar Berrospi Ramis, Vanessa López

IBM Research Europe

Dublin Lab, Ireland and Zurich Lab, Switzerland

t.l.hoang@ie.ibm.com, marco.sbodio@ie.ibm.com, Marcos.Martinez.Galindo@ibm.com

mykhaylo.zayats1@ibm.com, raulfd@ibm.com, victor.valls@ibm.com

gabriele.picco@ibm.com, ceb@zurich.ibm.com and vanlopez@ie.ibm.com

ABSTRACT

Recent research in representation learning utilizes large databases of proteins or molecules to acquire knowledge of drug and protein structures through unsupervised learning techniques. These pre-trained representations have proven to significantly enhance the accuracy of subsequent tasks, such as predicting the affinity between drugs and target proteins. In this study, we demonstrate that by incorporating knowledge graphs from diverse sources and modalities into the sequences or SMILES representation, we can further enrich the representation and achieve state-of-the-art results on established benchmark datasets. We provide preprocessed and integrated data obtained from 7 public sources, which encompass over 30M triples. Additionally, we make available the pre-trained models based on this data, along with the reported outcomes of their performance on three widely-used benchmark datasets for drug-target binding affinity prediction found in the Therapeutic Data Commons (TDC) benchmarks. Additionally, we make the source code for training models on benchmark datasets publicly available. Our objective in releasing these pre-trained models, accompanied by clean data for model pretraining and benchmark results, is to encourage research in knowledge-enhanced representation learning.

1 Introduction

Developing a concise representation of proteins and small molecules is a crucial task in AI-based drug discovery. Recent studies [22, 26] have focused on utilizing large databases of protein sequences or molecules for self-supervised representation learning. These representations are then fine-tuned using limited labeled data for tasks like predicting the binding affinity between drugs and targets. In the field of protein representation learning, [38] and [39] have demonstrated that enhancing protein representations with additional information from knowledge graphs, such as comprehensive textual data from the gene ontology [1], can enhance the performance of pre-trained representations on various protein properties and protein-protein interaction tasks.

While early results concerning knowledge-enriched representations for proteins show promise, there is a notable absence of openly available, carefully curated, integrated, and readily usable datasets in the research community for studying pre-training methods. This scarcity motivates us to preprocess datasets from diverse knowledge sources, incorporating abundant factual information and modalities, and make the data available alongside the pre-trained models, along with the prediction accuracy of downstream models. Our primary objective is to establish foundational datasets for research on multimodal knowledge-enhanced representation learning and evaluate the outcomes against established benchmarks for downstream tasks. In addition to presenting new state-of-the-art findings on standard benchmark datasets, we offer a comprehensive discussion that shares the insights gained during the creation of pretrained models, as well as the research challenges that must be overcome to develop knowledge-enhanced foundation models for therapeutic

sciences. The preprocessed datasets, pretrained models and the code for benchmark models training are open-sourced and available in our project github repository¹.

2 Multimodal knowledge representation learning

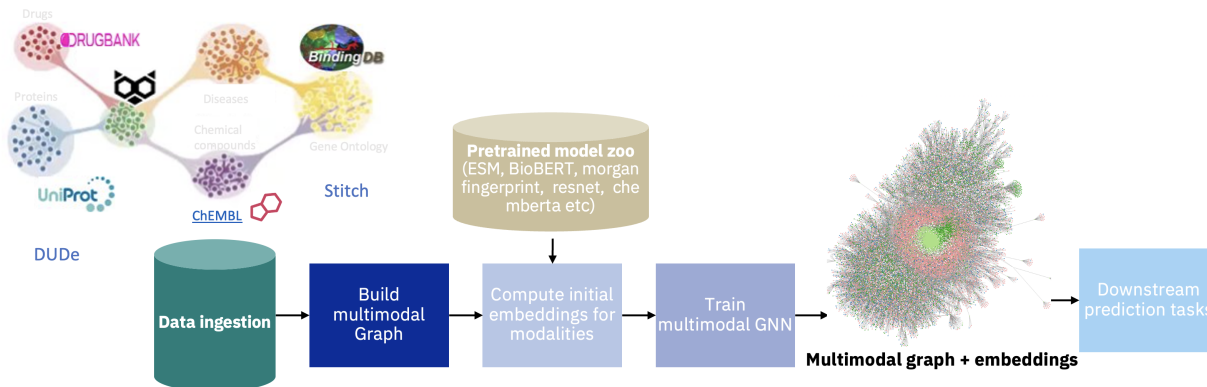


Figure 1: *Otter-Knowledge* workflow.

The diagram in Figure 1 illustrates the overall process of our system named *Otter-Knowledge*. This process involves constructing multimodal knowledge graphs from diverse sources, generating initial embeddings for each modality using pretrained models available in the model zoo, and subsequently improving the embeddings by incorporating information from the knowledge graphs through the utilization of graph neural networks (GNN).

2.1 Multimodal Knowledge graph construction

A Multimodal Knowledge Graph (MKG) is a directed labeled graph where labels have well-defined meanings, and each node has a modality, a particular mode that qualifies its type (text, image, protein, molecule, etc.). We consider two node subsets: *entity nodes* (or entities), which corresponds to concepts in the knowledge graph (for example protein, or molecule), and *attribute nodes* (or attributes), which represent qualifying attributes of an entity (for example the mass of a molecule, or the description of a protein). We refer to an edge that connect an entity to an attribute as *data property*, and an edge that connect two entities as *object property*. Each node in the graph has a unique identifier, and a unique modality (specified as a string).

We developed a framework for automating the construction of a multimodal knowledge graph by extracting and fusing data from a variety of sources, including text delimited files, JSON, and proprietary data sources [32]. The framework takes as input a schema file (specified in JSON), which declaratively describe how to build the desired graph from a set of data sources.

The framework that builds the MKG ensures that each triple is unique, and it automatically merges entities having the same unique identifier, but whose data is extracted from different data sources. It is also possible to use the special relation `sameAs`² to indicate that two entities having different unique identifiers are to be considered as the same entity. The `sameAs` relation is useful when creating a MKG from multiple partially overlapping data sources; when the graph is built. Additionally, it is possible to build an MKG incrementally, by merging two or more graphs built using different schemas; the merge operation automatically fuses entities having the same unique identifier or the same value of a distinctive attribute (for example the same sequence for two proteins).

The framework builds the graph in memory, but can also provide support for building the graph using a database on disk; the graph triples can also be serialised using GML³ or any RDF⁴ serialization formats. Finally, the framework provides scalable functionalities for parallel and GPU-based computation of the initial embedding vectors for the nodes; such embeddings are computed based on the modality of each node.

¹<https://github.com/IBM/otter-knowledge>

²We borrow the semantic of `owl:sameAs` - see <https://www.w3.org/TR/owl-ref/#sameAs-def>

³https://en.wikipedia.org/wiki/Graph_Modelling_Language

⁴<https://www.w3.org/RDF/>

2.2 Computing initial embeddings

As explained before, the MKG contains nodes representing entities and nodes representing attributes of those entities. In the MKG, each node has a modality assigned, e.g. entity nodes can have a modality *Protein* or *Drug*, nodes containing text could have a modality *text*. We assign a model for each one of the modalities in our graph, as specified by the user in the *schema*. The models, which we refer to as *handlers*, are capable of preprocessing the values in the nodes and computing their initial embeddings. Our framework allows to easily retrieve all the nodes in the graph with the same modality to efficiently compute the initial embeddings with the assigned *handler*, facilitating parallelization, GPU utilization, batching, and avoiding the need to load different models in memory simultaneously.

Some of these modalities do not have a *handler* assigned, like *Protein*, and therefore, no initial embedding is computed for them. For each modality, only one *handler* is being used, although it is possible to change the *handler* assigned. For instance, for SMILES it is possible to use *morgan-fingerprint* or *MolFormer*. These are the *handlers* that we have used for computing the initial embeddings of the graph:

- *morgan-fingerprint* We use the Morgan fingerprint in RDKit⁵ for processing the SMILES. Specifically, we use *GetMorganFingerprintAsBitVect*. We use by default a shape (also known as nBits or size) of 2048, and a radius of 2. If RDKit is not able to get the Morgan fingerprint of the SMILES we return an embedding of the same shape full of zeros.
- *MolFormer* [27] is a large-scale chemical language model designed with the intention of learning a model trained on small molecules which are represented as SMILES strings. *MolFormer* leverages Masked Language Modeling and employs a linear attention Transformer combined with rotary embeddings.
- *protein-sequence-mean* For the protein sequences, we use *esm1b_t33_650M_UR50S* [26]. We use the 33rd layer as representation layer, and compute the mean for the contacts. For the *batch_converter* we use *truncation_seq_length = 1022*.
- *text* For the textual values, we use the ‘sentence-transformers/paraphrase-albert-small-v2’ [24] model available in the Huggingface Hub⁶.
- *number* In the case of numbers, we do not use any model to get initial embeddings. We convert the numerical value to a torch tensor and use it as embedding.

2.3 Pretraining with inductive R-GNN

GNN architecture To improve representations of MKG entities we assimilate initial embeddings with the information about the MKG structure, i.e., connection patterns between graph nodes. To this end we train a Graph Neural Network (GNN) [40] that propagates initial embeddings through a set of layers that upgrade input embedding according to the node neighbours. The architecture of GNN consists of two main blocks: encoder and decoder. For encoder we first define a projection layer which consists of a set of linear transformations for each node modality and projects nodes into common dimensionality, then we apply several multi-relational graph convolutional layers (R-GCN) [29] which distinguish between different types of edges between source and target nodes by having a set of trainable parameters for each edge type. For decoder we consider link prediction task, which consists of a scoring function that maps each triple of source and target nodes and the corresponding edge and maps that to a scalar number defined over interval $[0; 1]$. Decoder and scoring function, and details about the hyperparameters are reported in the Appendix.

Learning objective For link prediction, we consider three choices of scoring functions: DistMult, TransE and a Binary Classifier that are commonly used in the literature. The outcomes of scoring of each triple are then compared against actual labels using negative log likelihood loss function. Certain pretraining datasets, like Uniprot, contain numerical data properties. Hence, we incorporate an extra regression objective aimed at minimizing the root mean square error (MSE) of the predicted numerical data properties. In the learning process, we combine the regression objective and the link prediction objective to create a single objective function.

Negative sampling We note that to train GNN with link prediction we need to provide network with both positive and negative examples. While positive examples come from the MKG itself, negative triples are generated synthetically. For this for each relation type we extract a set of admissible source and target nodes and then we randomly sample source and target from the corresponding admissible sets. We use an equal ratio between positive and negative links in the pretraining.

⁵<https://www.rdkit.org/docs/index.html>

⁶<https://huggingface.co/sentence-transformers/paraphrase-albert-small-v2>

Datasets	# triples	Entities	Modalities	Data license	Released
UBC	6,207,654	Pro teins/Drugs	sequences, SMILES text, number, category	Open	Yes
PrimeKG	12,757,257	Proteins/Drugs/ Diseases	sequences, SMILES text	Open	Yes
DUDe	40,216	Proteins/Drugs	sequences, SMILES	Open	Yes
STITCH	12,621,873	Proteins/Chemicals	sequences, SMILES	Open	Yes

Table 1: Summary of the KGs for pretraining models with the number of triples used for GNN training. More details on the modalities, entities and data properties are discussed in the Appendices.

Scaling the GNN training Due to the integration of data from various sources, the size of the integrated data can become quite large. For instance, the combination of Uniprot, ChEMBL, and BindingDB necessitates over 200GB of CPU memory for training. However, training a graph neural network (GNN) on such a massive graph using limited GPU memory is highly inefficient. To address this, we employ a graph auto-scaling approach (GAS) described in the reference [8]. This method divides the graph into smaller partitions using Metis⁷. GAS performs training on each partition separately, so it is able to scale to arbitrarily large graphs. To avoid information loss due to the connection between partitions, it keeps node embeddings of previous training step in CPU memory thus saving GPU memory during training and uses this historical embeddings to update the nodes inside a partition. Please refer to Appendix for details about the hyper-parameter settings of GAS.

Information flow control and noisy link prediction One crucial aspect of pretraining the GNN involves addressing the disparity between the data accessible during pretraining and the data accessible during subsequent tasks. Specifically, during pretraining, there are numerous attributes associated with proteins or drugs, whereas during downstream fine-tuning, only amino acid sequences and SMILES are available. Consequently, during pretraining, we explore two scenarios: one which controls the information propagated to the Drug/Protein entities and one without such control. In our experiments, we present results for both cases to provide an insight on the impact of restricting information flow during pretraining on the subsequent tasks. An additional significant consideration is the presence of noisy links within the up-stream data and how they affect the downstream tasks. To investigate the potential impact on these tasks, we manually handpick a subset of links from each database that are relevant to drug discovery (see details in the Appendix). We then compare the outcomes when training the GNN using only these restricted links versus using all possible links present in the graphs.

3 Pretraining datasets collections

Table 1 summarises the pretrained datasets. In this subsection, we discuss data preprocessing methods. For details about datasets and schema, readers can refer to the appendices and the github repository.

Uniprot [5] comprises of 573,227 proteins from SwissProt, which is the subset of manually curated entries within UniProt, including attributes with different modalities like the sequence (567,483 of them), full name, organism, protein family, description of its function, catalytics activity, pathways and its length. The number of edges are 38,665 of type *target_of* from Uniprot ids to both ChEMBL and Drugbank ids, and 196,133 interactants between Uniprot protein ids.

BindingDB [16] consists of 2,656,221 data points, involving 1.2 million compounds and 9,000 targets. Instead of utilizing the affinity score, we generate a triple for each combination of drugs and proteins. In order to prevent any data leakage, we eliminate overlapping triples with the TDC DTI dataset. As a result, the dataset concludes with a total of 2,232,392 triples.

ChEMBL [9] comprises of drug-like bioactive molecules, 10,261 ChEMBL ids with their corresponding SMILES were downloaded from OpenTargets [18], from which 7,610 have a *sameAs* link to drugbank id molecules.

Drugbank [13] comprises of detailed chemical data on 9,749 drugs (such as SMILES, description, indication, mechanism of action, affected organism, average mass, toxicity, calculated and experimental properties, absorption), classification, drug pathways and 1,301,422 drug interactions

⁷<https://github.com/KarypisLab/METIS>

Datasets	DTI DG	DAVIS	KIBA
# triples	232460	27621	118036
# drugs	140745	68	2068
# proteins	569	379	299
Type of splits	Temporal	Random/Drug/Target	Random/Drug/Target

Table 2: TDC benchmark datasets and statistics.

DUDe [17] comprises a collection of 22,886 active compounds and their corresponding affinities towards 102 targets. For our study, we utilized a preprocessed version of the DUDe [31], which includes 1,452,568 instances of drug-target interactions. To prevent any data leakage, we eliminated the negative interactions and the overlapping triples with the TDC DTI dataset. As a result, we were left with a total of 40,216 drug-target interaction pairs.

PrimeKG (the Precision Medicine Knowledge Graph) [4] integrates 20 biomedical resources, it describes 17,080 diseases with 4 million relationships. PrimeKG includes nodes describing Gene/Proteins (29,786) and Drugs (7,957 nodes). The MKG that we built from PrimeKG contains 13 modalities, 12,757,300 edges (154,130 data properties, and 12,603,170 object properties), including 642,150 edges describing interactions between proteins, 25,653 edges describing drug-protein interactions, and 2,672,628 describing interactions between drugs.

STITCH (Search Tool for Interacting Chemicals) [34] is a database of known and predicted interactions between chemicals represented by SMILES strings and proteins whose sequences are taken from STRING database [33]. Those interactions are obtained from computational prediction, from knowledge transfer between organisms, and from interactions aggregated from other (primary) databases. For the MKG curation we filtered only the interaction with highest confidence, i.e., the one which is higher 0.9. This resulted into 10,717,791 triples for 17,572 different chemicals and 1,886,496 different proteins. Furthermore, the graph was split into 5 roughly same size subgraphs and GNN was trained sequentially on each of them by upgrading the model trained using the previous subgraph.

4 Experiments

We summarise the main results from our experiments and further details are available in the appendices.

4.1 Results and discussion

4.2 Benchmark tasks and downstream models

Downstream benchmarks We use the TDC [12] benchmark datasets regarding drug-target binding affinity for evaluation. The DTI-DG dataset has a leaderboard with the state-of-the-art metrics reported for different methods. The data was temporally split based on patent application dates making this dataset suitable for method generalization evaluation. On the other hand, the DAVIS and the KIBA datasets have a random split, together with two more splits based on target or drug. The latter splits help validate the learning methods against new drugs/proteins never seen during training.

Downstream models The TDC framework adapts the DeepDTA framework [21] to learn drug/protein features using separated convolution layers before concatenating transformed features for binding affinity prediction. We discovered that the given architecture is not effective in the context where both drug and protein embeddings are already given as input. With the original TDC framework, the baseline used in Table 3, based on ESM embeddings for proteins and Morgan fingerprints for molecules SMILES, gives much worse results (0.539) than using an architecture that directly concatenates protein and drug embeddings for further transformation (0.569) on the DTI DG dataset. Therefore, we create a new model architecture for the evaluation of the pretrained embeddings. Besides the network that transforms the ESM and Morgan fingerprint, we create a parallel network that transforms the GNN embeddings. Both networks predict the binding affinity and the final prediction is the sum of two predictions (for details about the network size refer to the Appendices).

Ensemble learning The pretrained representation is sensitive to various factors, such as the chosen objectives for the Graph Neural Network (GNN) and the specific graphs used for training. Additionally, combining all the datasets into a single large graph requires substantial computational resources and poses challenges in aligning different databases. In this study, we propose a simple approach that involves combining pretrained embeddings obtained from different settings and datasets. This allows us to train multiple GNN models simultaneously without the need to merge all the

Upstream	Downstream Splits	DTI DG			DAVIS			KIBA		
		Temporal	Random	Target	Drug	Random	Target	Drug		
	Leaderboard ⁸	0.538	NA	NA	NA	NA	NA	NA		
	Baseline	0.569	0.805	0.554	0.264	0.852	0.630	0.576		
UBC	Otter DistMult	0.578	0.808	0.572	0.152	0.859	0.627	0.593		
	Otter TransE	0.577	0.807	0.571	0.130	0.858	0.644	0.583		
	Otter Classifier	0.580	0.810	0.573	0.104	0.861	0.631	0.616		
DUDe	Otter DistMult	0.577	0.805	0.573	0.132	0.857	0.650	0.607		
	Otter TransE	0.576	0.807	0.570	0.170	0.858	0.653	0.604		
	Otter Classifier	0.579	0.808	0.574	0.167	0.860	0.641	0.630		
PrimeKG	Otter DistMult	0.575	0.806	0.571	0.162	0.858	0.611	0.617		
	Otter TransE	0.573	0.807	0.568	0.186	0.858	0.642	0.607		
	Otter Classifier	0.576	0.813	0.576	0.133	0.861	0.630	0.635		
STITCH	Otter DistMult	0.575	0.808	0.573	0.138	0.859	0.615	0.603		
	Otter TransE	0.578	0.814	0.572	0.119	0.859	0.636	0.635		
	Otter Classifier	0.576	0.804	0.571	0.156	0.856	0.627	0.585		
	Otter Ensemble	0.588	0.839	0.578	0.168	0.886	0.678	0.638		

Table 3: Results of knowledge enhanced representation on three standard drug-target binding affinity prediction benchmarks datasets with different splits. The evaluation metrics is Pearson correlation (higher is better). We reported the results concerning pretraining on separate upstream datasets and the ensemble of these models.

Datasets (UBC) Splits	DTI DG			DAVIS			KIBA		
	Temporal	Random	Target	Drug	Random	Target	Drug		
Otter DistMult (C)	0.575	0.809	0.571	0.126	0.861	0.643	0.617		
Otter TransE (C)	0.576	0.809	0.570	0.157	0.858	0.632	0.585		
Otter Classifier (C)	0.578	0.814	0.577	0.097	0.861	0.633	0.631		
Otter DistMult (N+C)	0.578	0.809	0.574	0.105	0.862	0.643	0.615		
Otter TransE (N+C)	0.579	0.809	0.573	0.108	0.857	0.633	0.583		
Otter Classifier (N+C)	0.580	0.816	0.577	0.147	0.864	0.639	0.641		
Otter DistMult (N+C+R)	0.579	0.810	0.572	0.145	0.862	0.629	0.625		
Otter TransE (N+C+R)	0.580	0.811	0.576	0.073	0.859	0.627	0.594		
Otter Classifier (N+C+R)	0.582	0.812	0.574	0.124	0.860	0.619	0.600		

Table 4: Information flow control and noisy links results for UBC for different scoring functions. The table results should be compared with the results in Table 3 (UBC). The evaluation metrics is Pearson correlation (higher is better). N (noisy links); C (no flow control); R (regression).

datasets into a single location, resulting in savings in computational resources and effort required for database alignment. We create a linear ensemble by assigning equal weights to individual downstream models, each trained with separate pretrained embeddings given by individual GNN models.

Knowledge enhanced representation versus vanilla representation In Table 3, we present the outcomes of the *Otter-Knowledge* models, which were pretrained on graphs generated from Uniprot (U), BindingDB (B), ChemBL (C), DUDe, PrimeKG and STITCH with three different training objectives: TransE, DistMult, and binary classifier respectively. Also, and as described in Section 2.3, we control the information propagated to the Drug/Protein entities, and manually handpick a subset of links from each database that are relevant to drug discovery. In all of these methods, we started with the initial embeddings of sequences using ESM-1b models, and Morgan fingerprints were utilized for SMILES, we call this baseline method vanilla representation as oppose to methods with knowledge enhanced representation. The embeddings were then fine-tuned with knowledge graphs. Our results demonstrate that *Otter-Knowledge* outperforms the baseline vanilla representation without the enhanced knowledge from the graphs. Notably, a significant improvement was observed when we created an ensemble of 12 models trained on UDC and DUDe, PrimeKG and STITCH. We achieved state-of-the-art (SOTA) results on the leaderboard of the DTI DG dataset. However, for the KIBA dataset with drug split, the improvements were not substantial. As indicated in Table 4, the KIBA dataset consists of only 68 drugs. The limited number of drugs makes this specific split particularly challenging, and we consider it an open challenge for future research.

Information flow and noisy links Table 4 shows the results of *Otter-Knowledge* for UBC when (i) we do *not* control the information that is propagated to Drug/Protein entities, (ii) we do *not* cherry-pick a subset of links from each database that are relevant to the downstream task, (iii) regression for numerical data properties is added to the

Datasets	DTI DG		DAVIS		KIBA		
Splits	Temporal	Random	Target	Drug	Random	Target	Drug
MolFormer	0.547	0.811	0.578	0.103	0.838	0.642	0.624
Morgan fingerprint	0.574	0.806	0.573	0.125	0.861	0.631	0.619

Table 5: Impact of different modalities for drugs on the UDB datasets

objective in addition to link prediction. Observe from the table that the results are similar to the results in Table 3, with minor variations across different scoring functions and datasets. Notably, Otter Classifier with noisy links (N) and no information flow control (C) achieves comparable or even better performance than when we cherry-pick links and control the flow of information (Table 3). These minor variations suggest that the embeddings computed by the GNN are resilient to noisy triples that are not directly relevant to the downstream tasks. Adding regression objectives and information flow control does not provide a significant result improvement.

Morgan-fingerprint versus MolFormer The base of the *Otter-Knowledge* is to leverage the pre-trained representations, before enhancing them with additional knowledge. Thus, the initial embeddings computed for the SMILES and sequences have an impact in the results. Table 5 shows the results of *Otter-Knowledge* using a ClassifierHead, trained on UDB for 25 epochs with different drug initial representations. We can see that the MolFormer does not give superior results compared to Morgan-fingerprint, there is room for improvement regarding learned representation over simple fingerprint-based approaches for small molecules.

5 Related work

We review methods to learn an effective representation from proteins, molecules and their interactions.

Representation learning for proteins and small molecules Representation learning focuses on encoding essential information about entities, such as proteins or molecules, into low-dimensional tensors. Self-supervised algorithms using language models (LMs) have achieved remarkable success in learning protein and molecule representations by training on extensive datasets of protein sequences or linear serialization of small molecules, such as SMILES. State of the art examples of transformer-based protein language models (PLMs) are TAPE [22], ProteinLM [36], ProteinBERT [2], ESM [25], Prottrans [6], and MSA [23]. They are typically trained on masked reconstruction – they learn the likelihood that a particular amino acid appears in a sequence context. Because the probability that a residue will be conserved or not across related sequences is intrinsically tied to its biological role, existent PLMs can capture co-evolutionary and inter-residue contact information [22, 25], and have shown impressive performance on various tasks, such as predicting protein structure [15] and function [22]. Regarding small molecules, their molecular structure can be condensed into linear notations like SMILES or SELFIES. LMs have also been used to interpret these representations, e.g., MolFormer [28], MolBERT [7], SmilesFormer [20] or SELFormer [37]. Both Protein and molecular representations have been fine-tuned using a contrastive learning co-embedding by Complex [30] achieving good performance in Drug-Target Interaction (DTI) prediction, surpassing state of the art approaches in the TDC-DG leaderboard which evaluates of out-of-domain generalisation [11] and achieving high specificity while detecting false positive bindings in “decoy” datasets like DUD-E.

Knowledge enhanced pre-trained language models for proteins LMs do not consider existent extensive knowledge, in the form of manually curated functional and structural annotations, in human-curated domain knowledge bases and effectively leveraging all this available factual knowledge to enhance representation learning is still an open research challenge. Nonetheless, prior research indicates that it can improve results in downstream learning tasks. OntoProtein [38] fine-tuned a PLM by reconstructing masked amino acids while minimizing the embedding distance between the contextual representation of proteins and associated gene ontology functional annotations [3]. For this purpose they built ProteinKG25, a KG consisting of 600k protein sequences and nearly five million triples. Their results show that the representations obtained were useful for classification tasks such as protein-protein interaction type, protein function, and contact prediction; but underperformed in regression tasks like homology, fluorescence, and stability.

KeAP [39], on the other hand, claims to explore a more granular token-level approach, where non-masked amino acids iteratively query the associated knowledge tokens to extract helpful information (from the Gene ontology) for restoring masked amino acids via cross-attention. The training process is guided only by the mask token reconstruction objective, while OntoProtein uses both contrastive learning and masked modelling simultaneously. KeAP, also trained on ProteinKG25 [38] and it outperforms OntoProtein on 9 downstream tasks, including contact, protein-protein interaction type, homology, stability, and protein-protein binding affinity prediction.

Graph-based approaches for therapeutics Graphs are a natural way to represent molecular interactions, signalling pathways, and disease co-morbidities. They can also be used for representation learning as they allow for the distillation of high-dimensional information about a node’s neighborhood into low-dimensional vector spaces. The training objective of these representations is that similar neighborhoods are embedded close to each other in the vector space. Optimised representations can then be used to train downstream models to predict properties of specific nodes (e.g., protein function), as well as, novel associations between nodes (e.g., drug-target interactions). An overview on graph representation learning in biomedicine can be found in [14]. State of the art approaches have shown that incorporating multiple knowledge sources improves downstream performance (e.g., DTiGEMS+ [35] formulates the prediction of DTIs as a link prediction problem in an heterogeneous graph, or TxGNN for predicting drug indications/contraindications for rare diseases [10]).

6 Conclusion and future work

In this paper, we study the representation learning problems for multimodal knowledge graphs fused from multiple sources. Our study serves as a foundation for future investigations in this area with the release of curated datasets from different sources in the format that is ready for studying pretraining methods. Additionally, we have made available pre-trained models that have been constructed using a comprehensive collection of open data. These models can be utilized to acquire representations specifically tailored for drug discovery applications. Furthermore, they can serve as benchmarks for comparing and evaluating against other baseline representation learning techniques. We have also made the standard evaluation framework for assessing pretrained representations in drug-target binding affinity prediction publicly available. Furthermore, we conducted a thorough analysis of various representation learning methods using three well-established benchmark datasets for drug-target binding affinity prediction. Notably, our approach achieved state-of-the-art results on the TDC DG dataset, demonstrating its superiority over existing methods.

Our study establishes the foundation for exploring the learning of multi-modal knowledge representation. Nevertheless, numerous unresolved research questions persist. Firstly, the incorporation of additional modalities, such as the 3D structure of molecules or proteins, can provide valuable insights for representation learning. Secondly, the challenge lies in effectively handling a vast number of databases, where aligning them is not a straightforward task. Developing a learning approach capable of accommodating the dynamic input schema from diverse sources is a crucial problem to address. Finally, evaluating generability of the learned graph representation for further (predictive or generative) downstream tasks and use cases and having a more robust learning methods for generalizing the learned representation to multiple tasks under data distribution shift is an important research topic.

7 Limitations

Due to license restriction of some datasets we only release the datasets with non-commercial licenses and the pretrained models that were built on these datasets. The datasets do not include 3D structure of proteins/drugs which can be an interesting modalities for future work.

References

- [1] M. Ashburner, C. A. Ball, J. A. Blake, D. Botstein, H. Butler, J. M. Cherry, A. P. Davis, K. Dolinski, S. S. Dwight, J. Eppig, M. A. Harris, D. P. Hill, L. Issel-Tarver, A. Kasarskis, S. E. Lewis, J. C. Matese, J. E. Richardson, M. Ringwald, G. M. Rubin, and G. Sherlock. Gene ontology: tool for the unification of biology. *Nature Genetics*, May 2000.
- [2] N. Brandes, D. Ofer, Y. Peleg, N. Rappoport, and M. Linial. ProteinBERT: a universal deep-learning model of protein sequence and function. *Bioinformatics*, 38(8):2102–2110, 02 2022.
- [3] G. Central, S. A. Aleksander, J. Balhoff, S. Carbon, J. M. Cherry, H. J. Drabkin, D. Ebert, M. Feuermann, P. Gaudet, N. L. Harris, et al. The gene ontology knowledgebase in 2023. *Genetics*, 224(1), 2023.
- [4] P. Chandak, K. Huang, and M. Zitnik. Building a knowledge graph to enable precision medicine. *Nature Scientific Data*, 2023.
- [5] T. U. Consortium. UniProt: the Universal Protein Knowledgebase in 2023. *Nucleic Acids Research*, 51(D1):D523–D531, 11 2022.
- [6] A. Elnaggar, M. Heinzinger, C. Dallago, G. Rehawi, Y. Wang, L. Jones, T. Gibbs, T. Feher, C. Angerer, M. Steinegger, D. Bhowmik, and B. Rost. Prottrans: Towards cracking the language of life’s code through self-supervised deep learning and high performance computing. *CoRR*, abs/2007.06225, 2020.

- [7] B. Fabian, T. Edlich, H. Gaspar, M. Segler, J. Meyers, M. Fiscato, and M. Ahmed. Molecular representation learning with language models and domain-relevant auxiliary tasks. *arXiv preprint arXiv:2011.13230*, 2020.
- [8] M. Fey, J. E. Lenssen, F. Weichert, and J. Leskovec. Gnnautoscale: Scalable and expressive graph neural networks via historical embeddings. In *International Conference on Machine Learning*, pages 3294–3304. PMLR, 2021.
- [9] A. Gaulton, L. J. Bellis, A. P. Bento, J. Chambers, M. Davies, A. Hersey, Y. Light, S. McGlinchey, D. Michalovich, B. Al-Lazikani, and J. P. Overington. ChEMBL: a large-scale bioactivity database for drug discovery. *Nucleic Acids Research*, 40(D1):D1100–D1107, 09 2011.
- [10] K. Huang, P. Chandak, Q. Wang, S. Havaladar, A. Vaid, J. Leskovec, G. Nadkarni, B. Glicksberg, N. Gehlenborg, and M. Zitnik. Zero-shot prediction of therapeutic use with geometric deep learning and clinician centered design. *medRxiv*, 2023.
- [11] K. Huang, T. Fu, W. Gao, Y. Zhao, Y. Roohani, J. Leskovec, C. Coley, C. Xiao, J. Sun, and M. Zitnik. Therapeutics data commons: Machine learning datasets and tasks for drug discovery and development. In J. Vanschoren and S. Yeung, editors, *Proceedings of the Neural Information Processing Systems Track on Datasets and Benchmarks*, volume 1. Curran, 2021.
- [12] K. Huang, T. Fu, W. Gao, Y. Zhao, Y. Roohani, J. Leskovec, C. W. Coley, C. Xiao, J. Sun, and M. Zitnik. Artificial intelligence foundation for therapeutic science. *Nature chemical biology*, 2022.
- [13] V. Law, C. Knox, Y. Djoumbou, T. Jewison, A. C. Guo, Y. Liu, A. Maciejewski, D. Arndt, M. Wilson, V. Neveu, A. Tang, G. Gabriel, C. Ly, S. Adamjee, Z. T. Dame, B. Han, Y. Zhou, and D. S. Wishart. DrugBank 4.0: shedding new light on drug metabolism. *Nucleic Acids Research*, 42(D1):D1091–D1097, 11 2013.
- [14] M. M. Li, K. Huang, and M. Zitnik. Graph representation learning in biomedicine and healthcare. *Nature Biomedical Engineering*, pages 1–17, 2022.
- [15] Z. Lin, H. Akin, R. Rao, B. Hie, Z. Zhu, W. Lu, N. Smetanin, A. dos Santos Costa, M. Fazel-Zarandi, T. Sercu, S. Candido, et al. Language models of protein sequences at the scale of evolution enable accurate structure prediction. *bioRxiv*, 2022.
- [16] T. Liu, Y. Lin, X. Wen, R. N. Jorissen, and M. K. Gilson. Bindingdb: a web-accessible database of experimentally determined protein–ligand binding affinities. *Nucleic acids research*, 35(suppl_1):D198–D201, 2007.
- [17] M. M. Mysinger, M. Carchia, J. J. Irwin, and B. K. Shoichet. Directory of useful decoys, enhanced (dud-e): better ligands and decoys for better benchmarking. *Journal of medicinal chemistry*, 55(14):6582–6594, 2012.
- [18] D. Ochoa, A. Hercules, M. Carmona, D. Suveges, J. Baker, C. Malangone, I. Lopez, A. Miranda, C. Cruz-Castillo, L. Fumis, M. Bernal-Llinares, K. Tsukanov, H. Cornu, K. Tsirigos, O. Razuvayevskaya, A. Buniello, J. Schwartzenuber, M. Karim, B. Ariano, R. Martinez Osorio, J. Ferrer, X. Ge, S. Machlitt-Northen, A. Gonzalez-Uriarte, S. Saha, S. Tirunagari, C. Mehta, J. Roldán-Romero, S. Horswell, S. Young, M. Ghousaini, D. Hulcoop, I. Dunham, and E. McDonagh. The next-generation Open Targets Platform: reimagined, redesigned, rebuilt. *Nucleic Acids Research*, 51(D1):D1353–D1359, 11 2022.
- [19] D. Ochoa, A. Hercules, M. Carmona, D. Suveges, J. Baker, C. Malangone, I. Lopez, A. Miranda, C. Cruz-Castillo, L. Fumis, M. Bernal-Llinares, K. Tsukanov, H. Cornu, K. Tsirigos, O. Razuvayevskaya, A. Buniello, J. Schwartzenuber, M. Karim, B. Ariano, R. Martinez Osorio, J. Ferrer, X. Ge, S. Machlitt-Northen, A. Gonzalez-Uriarte, S. Saha, S. Tirunagari, C. Mehta, J. Roldán-Romero, S. Horswell, S. Young, M. Ghousaini, D. Hulcoop, I. Dunham, and E. McDonagh. The next-generation Open Targets Platform: reimagined, redesigned, rebuilt. *Nucleic Acids Research*, 51(D1):D1353–D1359, 11 2022.
- [20] J. Owoyemi and N. Medzhidov. Smilesformer: Language model for molecular design. 2023.
- [21] H. Öztürk, A. Özgür, and E. Ozkirimli. Deepdta: deep drug–target binding affinity prediction. *Bioinformatics*, 34(17):i821–i829, 2018.
- [22] R. Rao, N. Bhattacharya, N. Thomas, Y. Duan, P. Chen, J. Canny, P. Abbeel, and Y. Song. Evaluating protein transfer learning with tape. In H. Wallach, H. Larochelle, A. Beygelzimer, F. d'Alché-Buc, E. Fox, and R. Garnett, editors, *Advances in Neural Information Processing Systems*, volume 32. Curran Associates, Inc., 2019.
- [23] R. M. Rao, J. Liu, R. Verkuil, J. Meier, J. Canny, P. Abbeel, T. Sercu, and A. Rives. Msa transformer. In M. Meila and T. Zhang, editors, *Proceedings of the 38th International Conference on Machine Learning*, volume 139 of *Proceedings of Machine Learning Research*, pages 8844–8856. PMLR, 18–24 Jul 2021.
- [24] N. Reimers and I. Gurevych. Sentence-bert: Sentence embeddings using siamese bert-networks. In *Proceedings of the 2019 Conference on Empirical Methods in Natural Language Processing*. Association for Computational Linguistics, 11 2019.

- [25] A. Rives, J. Meier, T. Sercu, S. Goyal, Z. Lin, J. Liu, D. Guo, M. Ott, C. Zitnick, J. Ma, and R. Fergus. Biological structure and function emerge from scaling unsupervised learning to 250 million protein sequences. *Proceedings of the National Academy of Sciences of the United States of America*, 118(15), Apr. 2021.
- [26] A. Rives, J. Meier, T. Sercu, S. Goyal, Z. Lin, J. Liu, D. Guo, M. Ott, C. L. Zitnick, J. Ma, and R. Fergus. Biological structure and function emerge from scaling unsupervised learning to 250 million protein sequences. *PNAS*, 2019.
- [27] J. Ross, B. Belgodere, V. Chenthamarakshan, I. Padhi, Y. Mroueh, and P. Das. Large-scale chemical language representations capture molecular structure and properties. *Nature Machine Intelligence*, 4(12):1256–1264, 2022.
- [28] J. Ross, B. Belgodere, V. Chenthamarakshan, I. Padhi, Y. Mroueh, and P. Das. Molformer: Large scale chemical language representations capture molecular structure and properties. 2022.
- [29] M. Schlichtkrull, T. N. Kipf, P. Bloem, R. van den Berg, I. Titov, and M. Welling. Modeling relational data with graph convolutional networks. In A. Gangemi, R. Navigli, M.-E. Vidal, P. Hitzler, R. Troncy, L. Hollink, A. Tordai, and M. Alam, editors, *The Semantic Web*, pages 593–607, Cham, 2018. Springer International Publishing.
- [30] R. Singh, S. Sledzieski, L. Cowen, and B. Berger. Learning the drug-target interaction lexicon. *bioRxiv*, 2022.
- [31] S. Sledzieski, R. Singh, L. Cowen, and B. Berger. Adapting protein language models for rapid dti prediction. *bioRxiv*, pages 2022–11, 2022.
- [32] P. W. J. Staar, M. Dolfi, and C. Auer. Corpus processing service: A knowledge graph platform to perform deep data exploration on corpora. *Applied AI Letters*, 1(2):e20, 2020.
- [33] D. Szklarczyk, R. Kirsch, M. Koutrouli, K. Nastou, F. Mehryary, R. Hachilif, A. Gable, T. Fang, N. Doncheva, S. Pyysalo, P. Bork, L. J. Jensen, and C. von Mering. The string database in 2023: protein-protein association networks and functional enrichment analyses for any sequenced genome of interest. *Nucleic acids research*, 51(D1):D638–D646, 2023.
- [34] D. Szklarczyk, A. Santos, C. von Mering, L. J. Jensen, P. Bork, and M. Kuhn. Stitch 5: augmenting protein-chemical interaction networks with tissue and affinity data. *Nucleic acids research*, 44(D1):D380–D384, 2016.
- [35] M. Thafar, R. Olayan, H. Ashoor, S. Albaradei, V. Bajic, X. Gao, T. Gojobori, and M. Essack. Dtigems+: drug-target interaction prediction using graph embedding, graph mining, and similarity-based techniques. *Journal of Cheminformatics*, 12(1), July 2020. KAUST Repository Item: Exported on 2020-10-01 Acknowledged KAUST grant number(s): BAS/1/1606-01-01, BAS/1/1059-01-01, BAS/1/1624-01-01, FCC/1/1976-17-01, FCC/1/1976-26-01. Acknowledgements: The research reported in this publication was supported by the King Abdullah University of Science and Technology (KAUST).
- [36] Y. Xiao, J. Qiu, Z. Li, C. Hsieh, and J. Tang. Modeling protein using large-scale pretrain language model. *CoRR*, abs/2108.07435, 2021.
- [37] A. Yüksel, E. Ulusoy, A. Ünlü, G. Deniz, and T. Doğan. Selfformer: Molecular representation learning via selfies language models. *arXiv preprint arXiv:2304.04662*, 2023.
- [38] N. Zhang, Z. Bi, X. Liang, S. Cheng, H. Hong, S. Deng, Q. Zhang, J. Lian, and H. Chen. Ontoprotein: Protein pretraining with gene ontology embedding. In *International Conference on Learning Representations*, 2022.
- [39] H.-Y. Zhou, Y. Fu, Z. Zhang, B. Cheng, and Y. Yu. Protein representation learning via knowledge enhanced primary structure reasoning. In *The Eleventh International Conference on Learning Representations*, 2023.
- [40] J. Zhou, G. Cui, S. Hu, Z. Zhang, C. Yang, Z. Liu, L. Wang, C. Li, and M. Sun. Graph neural networks: A review of methods and applications. *AI Open*, 1:57–81, 2020.

A Appendix

A.1 Experimental settings for upstream/downstream tasks

The downstream models comprise of two parallel structures. In the first architecture, the initial embeddings of drugs and proteins, obtained using the Morgan-fingerprint and ESM-1b models, are concatenated. These embeddings undergo a transformation through two linear layers and RELU activation before predicting the binding affinity. The second architecture involves the concatenation of GNN embeddings of drugs and proteins. Similarly, these embeddings are transformed using two linear layers and RELU activation, followed by predicting the binding affinity.

To obtain the final prediction for the binding affinity, the outputs of the two parallel networks are summed. Initially, a simpler approach was attempted, which involved concatenating all initial embeddings and GNN embeddings of drugs and proteins, followed by transforming these embeddings using a single network. However, this approach did not yield significant results due to the correlation between GNN embeddings and the initial embeddings of drugs and proteins. All the hyperparameters for the downstream models are provided in Table 6.

Since the primary focus of the work is the demonstration of the value of enriched representation using diverse information sources, rather than the discovery of optimal neural network structures, we did not perform an automated search for architectures. Instead, we established the size of the GNN (Graph Neural Network) and downstream models as specified in Table 6. To ensure reliable results, we conducted multiple downstream experiments using six different random seeds ranging from 0 to 5, following the recommended approach outlined in the TDC work [11]. The reported figures in this paper are the average outcomes obtained from these experiments.

GNN models		Downstream models	
Hyperparameters	Values	Hyperparameters	Values
# graph partitions	100	Learning rate	5e-4 (5e-5 for TDC DG)
Learning rate	1e-5	# training steps	10000 (20000 for TDC DG)
# layers	2	Batch size	256
Projection size	64	# layers	2
Hidden size	128	Initial embedding hidden size	[1024, 512]
Output size	128	GNN embedding hidden size	[1024, 1024]
Train/val	0.9	Activation	RELU
Training epochs	35	Random seeds	0-5
Acivation	RELU	# runs	6
Random seeds	3000		
Max train time	24 hours		

Table 6: Hyperparameters setting for pretrained GNN models and downstream models

The results presented in Table 3 rely on pretrained models that have restricted the information they can access for Protein/Drug entities. These entities are only allowed to utilize amino acid sequences and smiles. Inference tasks follow the pretraining tasks to acquire pretrained GNN embeddings for drugs/proteins in the downstream tasks. Even so Table 4 shows that information flow controls to drugs/proteins is not necessary to achieve good performance on the downstream tasks.

Learning rate has an impact on the downstream tasks, especially for KIBA and DAVIS. Figure 2 and Figure 3 show the sensitivity of setting of learning rate and its impact on the downstream model performance. We have tried different value of learning rates including 5e-4, 5e-5 and 5e-6. The results reported in the paper are based on fixing the learning rate to 5e-4. This value is set as the default learning rate for both the baseline and proposed methods in the work.

A.2 Model release

We made available a total of 12 pretrained models that were utilized in our experiments, as indicated in Table 3. Additionally, we have provided the source code necessary for performing inference using these models. To utilize these pretrained models, users can utilize the inference API and provide new protein sequences or new smiles as input. The API will then return both the initial embeddings and the pretrained GNN embeddings for the given input.

Table 7 provides a summary of the models. Each model’s name reflects the dataset it was trained on and the scoring function employed during pretraining. For instance, the model otter_abc_transe denotes the one trained on the Uniprot, BindingDB, and ChemBL (UBC) dataset using the TransE scoring function. All models underwent training for either 35 epochs or within a maximum time frame of 24 hours.

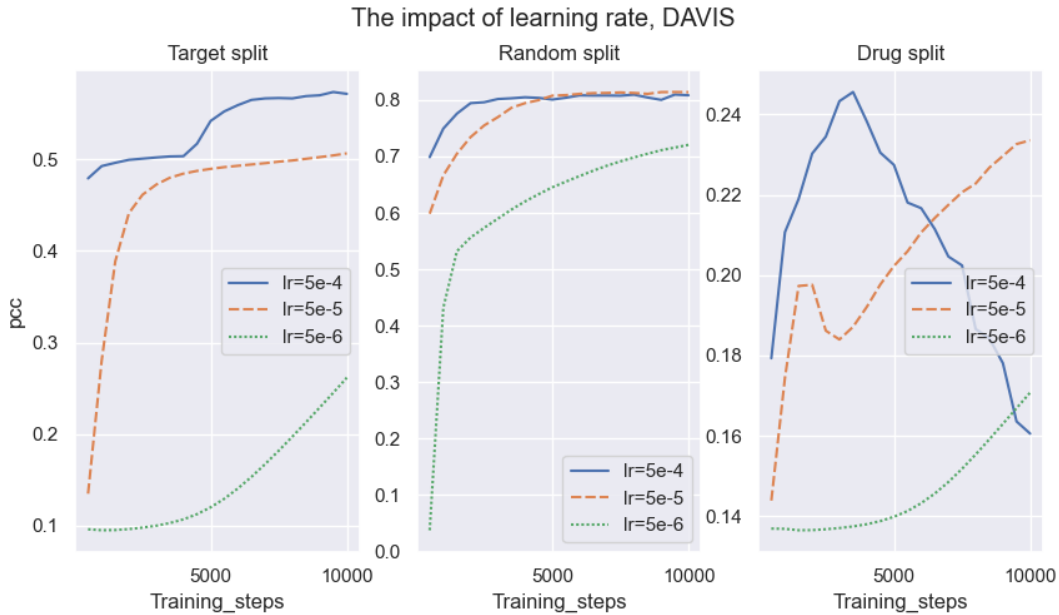


Figure 2: Learning rate impact on downstream DAVIS tasks

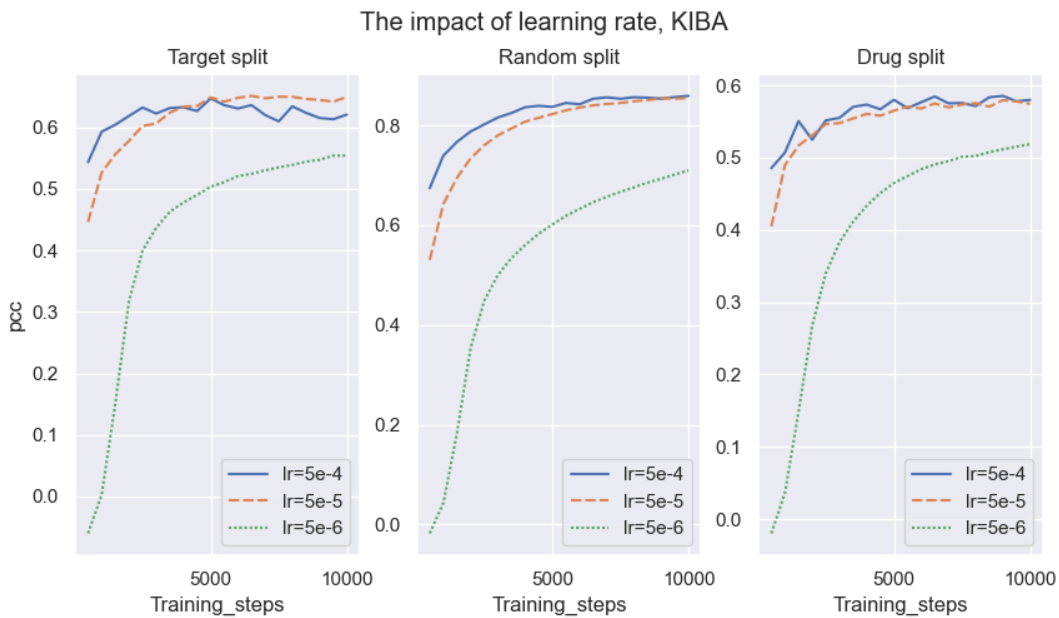


Figure 3: Learning rate impact on downstream KIBA tasks

The models can be found in the Huggingface hub ⁹. The name of the models in Table 7 is also the name of the models in the hub, under the IBM organization space. For example the otter_ubic_transe model could be found in the hub in https://huggingface.co/ibm/otter_ubic_transe.

A.3 Datasets release

We release the 4 KGs used to create the 12 pretrained models shown in (Table 7). The KGs were created from the original dataset sources using a JSON schema that specifies the type of entities and their namespaces; we use

⁹https://huggingface.co/models?sort=downloads&search=ibm/otter_

Models	Pretrain datasets	Learning objective	License
otter_abc_transe	UBC	TransE	MIT
otter_abc_distmult	UBC	DistMult	MIT
otter_abc_classifier	UBC	Classifier	MIT
otter_dude_transe	DUDe	TransE	MIT
otter_dude_distmult	DUDe	DistMult	MIT
otter_dude_classifier	DUDe	Classifier	MIT
otter_primekg_transe	PrimeKG	TransE	MIT
otter_primekg_distmult	PrimeKG	DistMult	MIT
otter_primekg_classifier	PrimeKG	Classifier	MIT
otter_stitch_transe	Stitch	TransE	MIT
otter_stitch_distmult	Stitch	DistMult	MIT
otter_stitch_classifier	Stitch	Classifier	MIT

Table 7: Summary of the released pretrained models.

namespaces to assign a unique identifier to each entity based on its source, so that we can connect them within and across dataset sources (an exception is PrimeKG, which requires custom processing of nodes because of the format of the original CSV files - we use however the same relations as defined by PrimeKG). For each entity type, the schema defines the relevant object and data properties and the modalities for both entities and attributes.

Figure 4 shows an example schema for the UBC KG, which comprises of 9,386,418 RDF triples obtained by combining factual information from Uniprot, BindingDB and a subset of ChEMBL Drugs molecules obtained from the Open Targets platform [19]; however for training the GNN we omitted triples with the `rdf:type` predicate, as this information is implicit in the modality and it would result in a very densely connected graph (e.g, when considering all nodes of type *Protein*), resulting in 6,207,654 triples. Figure 5 shows a portion of the resulting KG where an entity of type *Protein* defined with its UniProt ID and namespace (<https://www.uniprot.org/uniprot/P06820>) has data attributes such as sequence, label (Neuraminidase), family (glycosyl hydrolase 34 family), as well as object properties from and to other entities (e.g, a `target_of` relation to drug <https://go.drugbank.com/drugs/DB02268>, which is also the object of a `owl:sameAs` relation from https://www.ebi.ac.uk/chembl/target_report_card/CHEMBL1091644). We note that for STITCH the raw data was additionally processed to filter out interactions with the highest likelihood (> 0.9) and to remove duplicated interactions based on chemical SMILES and protein sequence. Also, files containing information about interactions, SMILES and protein sequences were joined into a single CSV file for which schema was designed for KG creation.

The datasets are serialised in N-Triples¹⁰, a line-based, plain text serialisation format for RDF triples and the pretrained models are accessible at¹¹. The original tabular datasets were either downloaded from their corresponding websites or accessed using IBM Deep Search¹², such as in the case of Uniprot SwissProt. Leveraging state-of-the-art AI methods, Deep Search collects, converts, enriches, and links large document collections [32] and it comes pre-loaded with millions of standard technical documents from many public data sources.

The same way as the models, the datasets can be found in the Huggingface hub. The names of the datasets in the hub, under the IBM organization space, are the next ones:

- `otter_uniprot_bindingdb`: (UB) MKG comprising entities and relations from Uniprot and BindingDB.
- `otter_uniprot_bindingdb_chembl`: (UBC) MKG comprising entities and relations from Uniprot, BindingDB and ChEMBL.
- `otter_dude`: (DUDe) MKG with data from the preprocessed version of DUDe
- `otter_primekg`: (PrimeKG) MKG with data from the PrimeKG
- `otter_stitch`: (STITCH) MKG with data from the preprocessed version of STITCH

Note that when training the GNN, the data attributes of a Protein or Drug entity node are treated as graph nodes with their own modalities (e.g textual, numerical, sequence, smiles), rather than considering them just as features or datatype attributes of the entity node. Therefore, the entity node (e.g, representing a Protein or Drug) receives information from the various available modalities through convolutional message passing in each iteration. The advantage is that entity

¹⁰<https://www.w3.org/TR/n-triples/>

¹¹<https://github.com/IBM/otter-knowledge>

¹²<https://ds4sd.github.io>

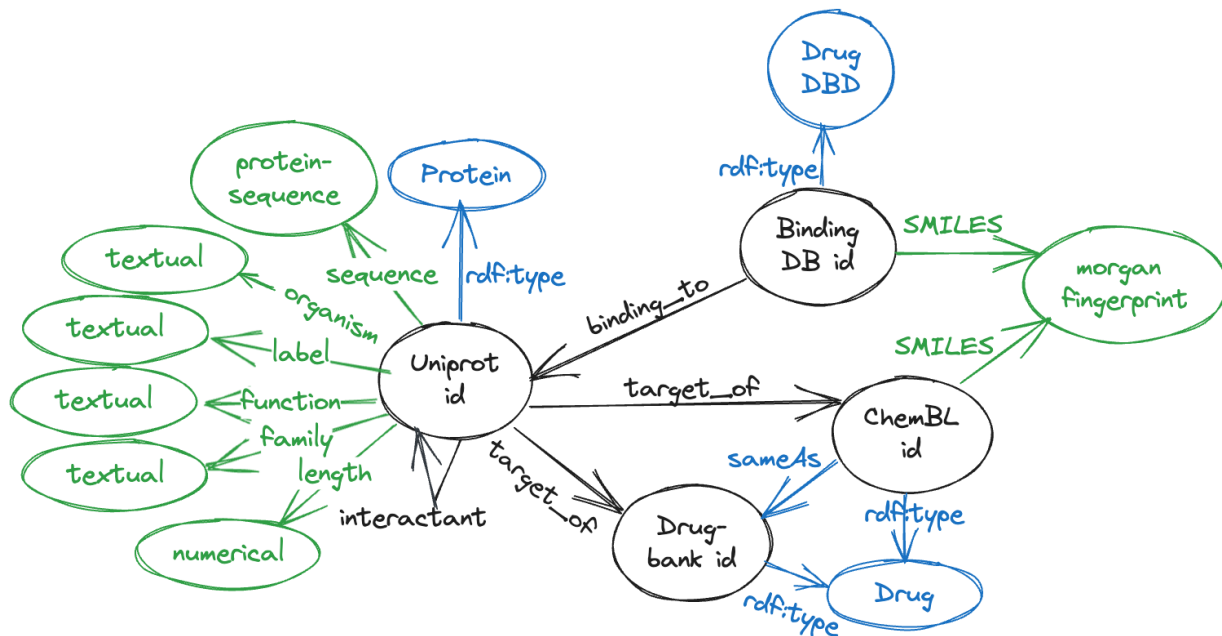


Figure 4: Schema for UBC Knowledge Graph.

Upstream	Downstream	DTI DG			DAVIS		KIBA	
		Splits	Temporal	Random	Target	Drug	Random	Target
UDB	Otter DistMult	0.577	0.809	0.571	0.144	0.858	0.636	0.587
	Otter TransE	0.581	0.805	0.571	0.132	0.857	0.633	0.585
	Otter Classifier	0.577	0.811	0.574	0.129	0.861	0.627	0.619
UB	Otter DistMult	0.576	0.808	0.574	0.126	0.858	0.627	0.596
	Otter TransE	0.579	0.808	0.571	0.162	0.858	0.633	0.581
	Otter Classifier	0.577	0.809	0.575	0.138	0.860	0.634	0.617

Table 8: Results of knowledge enhanced representation on three standard drug-target binding affinity prediction benchmarks datasets with different splits of the models pretrained with UDB and UB respectively.

nodes are not required to carry all multimodal properties or project large property vectors with missing values. Instead, the projection is done per modality and only when such a modality exists for the entity.

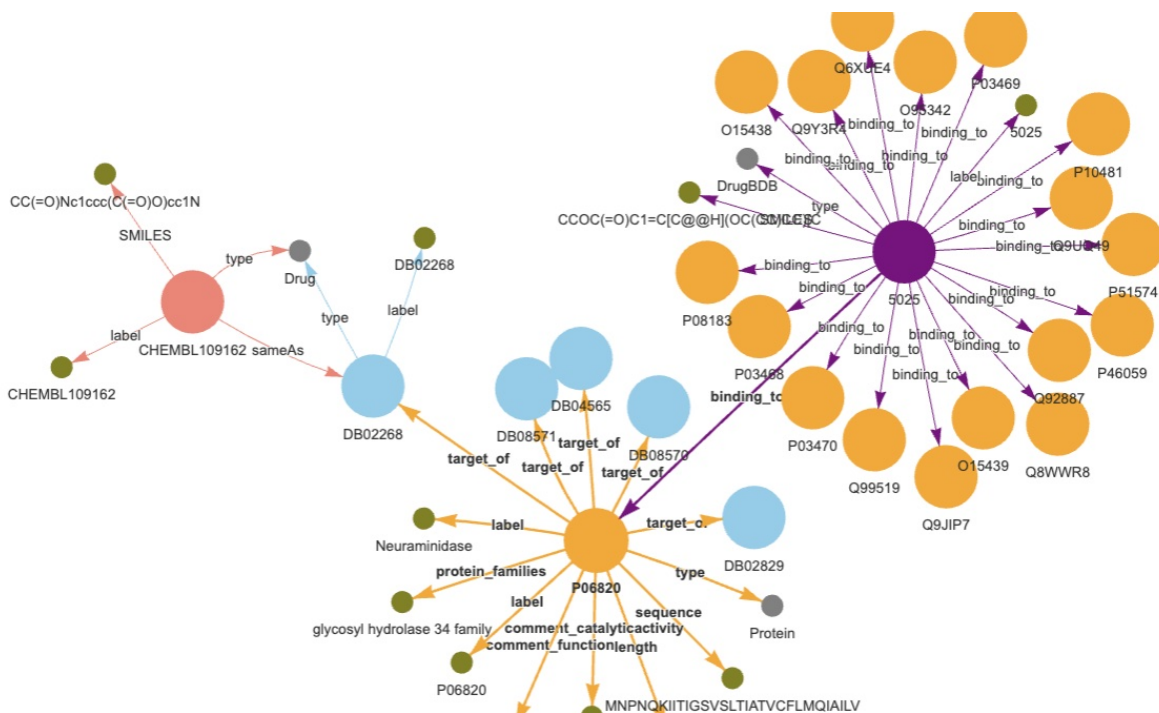
A.4 Results with UDB and UB

The outcomes of the model that underwent pretraining on Uniprot and BindingDB (UB) compared to the model that underwent pretraining on Uniprot, Drugbank, and BindingDB (UDB) are presented in Table 8. Although we are unable to share the processed Drugbank datasets because of licensing limitations, it is evident that incorporating Drugbank does not lead to significantly different results compared to using UB alone.

A.5 Computing resource and training time

Each pretrained model was trained using a single A100 GPU. The training process was restricted to a maximum duration of 24 hours and a maximum of 35 epochs for each pretraining graph. The specific number of epochs within the 24-hour time frame could differ based on the size of the input graph.

For managing the large graphs like the UBC, we utilized 200GB of CPU memory. The storage of the initial embeddings for the modality required the highest amount of memory compared to other components. With the implementation of the GAS methods explained in Section 2.3, the GNN training process was able to handle the large graphs effectively, even when constrained by GPU memory limitations.



Hydrolysis of alpha-(2->3)-, alpha-(2->6)-, alpha-(2->8)- glycosidic linkages of terminal sialic acid residues in oligosaccharides, glycoproteins, glycolipids, colominic acid and synthetic substrates. 1 to one round of replication. Described as a receptor-destroying enzyme because it cleaves a terminal sialic acid from the cellular receptors. May facilitate viral invasion of the upper airways by clea

Figure 5: Subset of a KG in UBC. Attribute nodes are coloured in green, type classes in blue, uniprot, chembl, drugbank and bindingDB entities are coloured in orange, salmon, blue and purple respectively

Datasets (UDB)	DTI DG		DAVIS			KIBA	
	Temporal	Random	Target	Drug	Random	Target	Drug
Otter DistMult (U)	0.576	0.811	0.574	0.143	0.857	0.642	0.580
Otter TransE (U)	0.576	0.807	0.573	0.147	0.857	0.641	0.581
Otter Classifier (U)	0.577	0.808	0.573	0.136	0.858	0.639	0.592
Otter DistMult (U+R)	0.576	0.809	0.573	0.141	0.859	0.635	0.597
Otter TransE (U+R)	0.575	0.808	0.574	0.145	0.858	0.634	0.596
Otter Classifier (U+R)	0.576	0.808	0.573	0.136	0.858	0.639	0.592
DistMult (N)	0.574	0.807	0.571	0.128	0.861	0.633	0.597
TransE (N)	0.573	0.812	0.575	0.178	0.862	0.633	0.596
Classifier (N)	0.579	0.808	0.575	0.141	0.860	0.638	0.603

Table 9: Universality results for UDB, where the scoring function considers all the knowledge graph links during the training. The table results should be compared with the results in Table 3 (UDB). The evaluation metrics is Pearson correlation (higher is better).

A.6 Downstream task open source

As we have discussed in Subsection 4.1, the neural architectures in the TDC framework are not optimal for the TDC DG benchmarks because they are designed to learn proteins/drugs representation from scratch. For pretrained proteins/drugs representation evaluation we created a new architecture that provide better results for both the baseline and the GNN representation. We made these architectures available for reproducible results. Additionally, we have open-sourced the source code of the ensemble methods used in our work.